Wnt1 Expression Temporally Allocates Upper Rhombic Lip Progenitors and Defines Their Terminal Cell Fate in the Cerebellum

Nellwyn Hagan[1] and **Mark Zervas**[2]

[1]Department of Neuroscience, Brown University, 70 Ship St., Providence, RI 02903

[2]Department of Molecular Biology, Cell Biology and Biochemistry, Division of Biology and Medicine, Brown University, 70 Ship St., Providence, RI 02903

Summary

The cerebellum (Cb) controls movement related physiology using a diverse array of morphologically and biochemically distinct neurons. During development, the Cb is derived from rhombomere 1 (r1), an embryonic compartment patterned by a signaling center referred to as the isthmus organizer. The secreted glycoprotein WNT1 is expressed in the midbrain primordia (mesencephalon, mes) and at the posterior limit of the mes, WNT1 plays a pivotal role in maintaining the isthmus organizer. Mutations in *Wnt1* produce severe Cb defects that are generally attributed to aberrant organizer activity. Interestingly, *Wnt1* is also expressed at the most posterior limit of dorsal r1, in a region known as the upper rhombic lip (URL). However, the distribution and molecular identity of *Wnt1* expressing progenitors have not been carefully described in r1. We used *Wnt1-Venus* transgenic mice to generate a molecular map of *Wnt1* expressing progenitors in relation to other well characterized Cb biomarkers such as MATH1 (ATOH1), LMX1a and OTX2. Our analysis validated *Wnt1* expression in the URL and revealed molecularly-defined developmental zones in r1. We then used genetic inducible fate mapping (GIFM) to link transient *Wnt1* expression in r1 to terminal cell fates in the mature Cb. *Wnt1* expressing progenitors primarily contributed to deep cerebellar nuclei, granule cells, and unipolar brush cells in distinct but overlapping temporal windows and sparsely contributed to inhibitory neurons and Bergmann glia. We further demonstrate that the *Wnt1* lineage does not follow a competency model of progressive lineage restriction to generate the Cb or the functionally related precerebellar system. Instead, progenitors initiate *Wnt1* expression *de novo* to give rise to each Cb cell type and precerebellar nuclei. We then used GIFM to determine how the temporal control of *Wnt1* expression is related to molecular identity and cell migration in Cb development. Our findings provide new insight into how lineage and timing establish cell diversity within the Cb system.

Keywords

Cerebellum; *Wnt1*; Genetic Inducible Fate Mapping; Lineage; Cell Fate; Mouse Genetics

---

Correspondence to: Mark Zervas.

Laboratory of Developmental Neurobiology, Genetics and Neurological Disease, Department of Molecular Biology, Cell Biology and Biochemistry, Division of Biology and Medicine, Box G-E436, Brown University, Providence, RI 02912, Courier delivery: Laboratories for Molecular Medicine, 70 Ship Street, Rm. 436, Providence, RI 02903, Mark_Zervas@brown.edu, Tel: 401-863-6840, Fax: 401-863-9653, Web page: http://research.brown.edu/myresearch/Mark_Zervas

Introduction

Wnt1 encodes a secreted glycoprotein that is expressed in spatially and temporally restricted domains during development and is important for patterning the mes and r1 (McMahon and Bradley, 1990). *Wnt1* expressing progenitors in the mes, marked at different embryonic time points, give rise to distinct dorsal and ventral midbrain (Mb) structures (Zervas et al., 2004; Ellisor et al., 2009). Lineage boundaries prevent *Wnt1* expressing progenitors in the mes from substantially populating r1 and r1 derivatives from contributing to dorsal Mb (Zervas et al., 2004; Sunmonu et al., 2011). At this boundary, *Wnt1* participates in a complex genetic loop that maintains the isthmus organizer, a signaling center critical for patterning both the mes and r1 (Liu and Joyner, 2001). The functional requirement for *Wnt1* is evident from *Wnt1*$^{-/-}$ mutant embryos which fail to develop a Mb and Cb and die perinatally (McMahon and Bradley, 1990). Similarly, mice with a naturally occurring point mutation in *Wnt1* (*Wnt1*$^{sw/sw}$) have severe Mb and Cb defects and only a small percentage escape lethality (Thomas et al., 1991). Currently, the Cb phenotypes of *Wnt1* mutants are attributed to aberrant signaling at the isthmus organizer (McMahon et al., 1992; Danielian and McMahon, 1996) or a perturbation in the mes/r1 lineage boundary (Bally-Cuif et al., 1995). Interestingly, *in situ* hybridization (ISH) shows that *Wnt1* is also expressed in the posterior domain of dorsal r1 beginning at E10.5 in the mouse (Wilkinson et al., 1987). This region, known as the URL, serves as a germinal zone for excitatory cell types of the Cb (Machold and Fishell, 2005; Wang et al., 2005). The presence of *Wnt1* expression in the URL raises the possibility that *Wnt1* shapes Cb development from within r1. Alternatively, *Wnt1* expressing cells could serve as a transient signaling center and subsequent to their role in patterning simply die off, similar to *Fgf8* expressing cells in the limb apical ectodermal ridge (Kimmel et al., 2000; Guo et al., 2003). Previous work indicated that the *Wnt1* lineage marked at E10.5 makes a very small contribution to the Cb (Zervas et al., 2004). However, this contribution was considered an ancillary observation and not explored in detail or pursued by marking at later time points. Using marker analysis, we showed that *Wnt1* is expressed in molecularly distinct domains in the URL from E10.5-E13.5 suggesting that *Wnt1* expressing progenitors arising from this domain are poised to make a significant contribution to the Cb. Our GIFM analysis established that *Wnt1* expressing progenitors in r1 do indeed contribute to an array of neuronal types in the Cb. Specifically, we observed a distinct rise, peak, and fall of the *Wnt1* lineage contribution to each excitatory Cb cell type. By temporally dissecting this contribution and following the developmental progression of the *Wnt1* lineage, we uncovered that *Wnt1* expression is induced *de novo* in r1 progenitors and corresponds with the order in which each Cb cell type emerges from the URL. However, the developmental profile of the *Wnt1* lineage demonstrated that the timing of *Wnt1* expression does not dictate when progenitors within a particular cell class will migrate away from the germinal zone. Our fate mapping analysis also revealed that lower rhombic lip (LRL) progenitors express *Wnt1* at similar embryonic stages as observed in the URL and differentially give rise to neurons of the precerebellar system, a major source of afferent projections to the Cb. Our genetic lineage tracing also reveals axons from *Wnt1*-derived neurons in the precerebellar system that innervate the Cb. The synchrony of *Wnt1* expression in the URL and LRL may coordinate the development of these two functionally related systems. In this regard, our study produces important information about the competency and development of the *Wnt1* lineage and the temporal windows in which *Wnt1* expressing progenitors give rise to distinct cell types in the Cb and precerebellar system.

Materials and Methods

Animals

Wnt1-Venus transgenic mice were generously provided by A. Joyner. Briefly, they were generated by subcloning a cassette encoding yellow fluorescent protein (*Venus*) into a multi-

cloning site between the translated and untranslated region of exon 1, which places *Venus* under the control of *Wnt1* regulatory elements (See Brown et al., 2011). This same configuration was successfully used to control *CreER^T* expression in *Wnt1-CreER^T* transgenic mice (Zervas et al., 2004). The *TOPGAL* (DasGupta and Fuchs, 1999), *Z/EG* (*tg(ACTB-lox-βGeo-lox-EGFP)*, (Novak et al., 2000)), and *Rosa26^tdTomato* (*Rosa26^lox-STOP-lox-tdTomato*, (Madisen et al., 2010)) reporter mice were purchased from Jackson Laboratories (stock # 004623, 003920, and 007908 respectively) and *mGFP* reporter mice (*Tau^lox-STOP-lox-mGFP-IRES-NLS-LacZ-pA*, (Hippenmeyer et al., 2005)) were generously provided by S. Arber. Mice were housed and handled in accordance with Brown University Institutional Animal Care and Use Committee guidelines. Genotyping was done as previously described (Ellisor et al., 2009; Brown et al., 2009, Jackson Laboratories website).

Wnt1-Venus Tissue Preparation

Wnt1-Venus transgenic mice were bred with Swiss Webster wildtype females (Taconic) to obtain litters at six different embryonic stages (E9.5-E14.5). Litters were dissected in PBS over ice and *Wnt1-Venus* embryos were identified by GFP fluorescence and confirmed by genotyping for GFP (Ellisor et al., 2009). Embryos were fixed in 4% PFA overnight at 4°C, cryoprotected, and embedded in OCT. Embryos (n=3 across two litters for each embryonic stage) were sectioned sagittally (12 μm) with a Leica cryostat and stored at −20°C.

Fate mapping Tissue Preparation

Fate mapping experiments were conducted by crossing *Wnt1-CreER^T;Rosa26^tdTomato*, *Wnt1-CreER^T;mGFP*, or *Wnt1-CreER^T;Z/EG* males with Swiss Webster wildtype females (Taconic). The morning (0900) of the day a vaginal plug was detected was designated as 0.5 days post-coitus. Tamoxifen was administered at a dose of 4 mg to timed pregnant females by oral gavage at 0900 (Brown et al., 2009; Ellisor and Zervas, 2010). Fate mapped tissue was collected at four endpoints (E14.5, E18.5, P7, P42) and tail samples were obtained from each mouse for genotyping. At E14.5 and E18.5, *Wnt1-CreER^T;Rosa26^tdTomato* fate mapped embryos were dissected, fixed, cryoprotected, embedded, and sectioned (12 μm and 20 μm respectively) as described above. At P7, *Wnt1-CreER^T;Rosa26^tdTomato* fate mapped mice were deeply anesthetized with Nembutal and intracardially perfused with 4% paraformaldehyde. Craniotomies were performed to extract the fate mapped brains, which were cryoprotected, embedded, and sectioned sagittally (20 μm) as previously described. At P42, *Wnt1-CreER^T;mGFP* and *Wnt1-CreER^T;Z/EG* mice were intracardially perfused as described for P7 mice. Craniotomies were performed to extract the fate mapped brains, which were then embedded in 3% agarose in PBS and sectioned sagittally (40 μm) with a Leica vibratome (Brown et al., 2009). Three fate mapped brains across two litters were processed for each marking and analysis stage.

In Situ Hybridization (ISH)

Both wildtype and *Wnt1-Venus* tissue sections were analyzed by ISH as previously described (Ellisor et al., 2009) with digoxigenin labeled probes for *Wnt1*, *GFP,* or *Math1* mRNA. The *Math1* mRNA probe was generously provided by S. Ahn. The *GFP* expression plasmid (*pGFP*) was generated by PCR amplifying a 600 bp fragment of GFP (using the GFP sense primer 5′-CTG GTC GAG CTG GAC GGC GAC G-3′ and anti-sense primer 5′-CAC GAA CTC CAG CAGGAC CAT G-3′) and sub-cloning this fragment into the pCR®II-TOPO® vector using a TA Cloning® Kit (Invitrogen, Cat # K2020-20). The anti-sense *GFP* ISH probe was made by digesting *pGFP* with SpeI and labeled with T7 polymerase and digoxigenin.

Immunocytochemistry (ICC)

Wnt1-Venus tissue sections from E10.5-E14.5 were analyzed by ICC with the following primary antibodies: anti-GFP (1:500, Nacalai Tesque Inc; Cat # GF090R), anti-OTX2 antibody (1:1000, gratefully obtained from S. Ang, NIMR, UK), anti-LMX1a antibody (1:1000, gratefully obtained from M. German, UCSF). The secondary antibodies, Alexa 555 (Invitrogen; Cat # A-31572; donkey anti-rabbit IgG) and Alexa 488 (Invitrogen; Cat # A-21208; donkey anti-rat IgG) were prepared at a concentration of 1:500. For fate mapping experiments, anti-β-galactosidase (β-gal, 1:500, Biogenesis, Cat # 4600-1409 and 1:500, Abcam, Cat # ab9361-250), anti-EGFP (1:600, Molecular Probes; Carlsbad, CA; Cat # A-11122 and 1:500, Nacalai Tesque Inc; Cat # GF090R), and anti-DsRed (1:500, Clontech, Cat # 632496) antibodies were used to identify *Wnt1*-derived cells. We also used anti-Calretinin (1:5000, Chemicon; Billerica, MA; Cat # AB1550), anti-Calbindin (1:1000, Swant, Cat # CB3a), anti-Parvalbumin (1:1000, Sigma, Cat # P3088-.2ML), and anti-Pax2 (1:50, Invitrogen, Cat # 71-6000) antibodies as biomarkers for different Cb cell types. The secondary antibodies, Alexa 555 (Invitrogen; Cat # A-31572, donkey anti-rabbit IgG; Cat # A21432, donkey anti-goat IgG), Dylight 549 (Jackson ImmunoResearch Laboratories; Cat # 703-505-155, donkey anti-chicken) and Alexa 488 (Invitrogen; Cat # A21208, donkey anti-rabbit IgG; Cat # A-21202 donkey anti-mouse IgG; Cat # A552222, donkey anti-goat IgG; Cat # A-21208; donkey anti-rat IgG) were prepared at 1:500. *Rosa26^{tdTomato}*, *mGFP*, and *Z/EG* littermates were immunolabled (anti-DsRed, anti-β-gal, and anti-EGFP antibodies respectively) to demonstrate that the reporter alleles were not leaky in their expression. Likewise, *Wnt1-CreER^T;Rosa26^{tdTomato}*, *Wnt1-CreER^T;mGFP*, and *Wnt1-CreER^T;Z/EG* mice that received only corn oil (as control for tamoxifen activation) did not show recombination.

Microscopy

Data were collected with a Leica DM600B epifluorescent microscope using Volocity 5.1 imaging software (Improvision). Low magnification images were captured with 2.5× and 5× objectives and high magnification images were obtained using a motorized stage with 10×, 20×, or 40× objectives. True magnifications are indicated by scale bars. All images were pseudo colored live as part of the acquisition palettes. In the 3D module of Volocity 5.1, 3-dimensional renderings were generated from a z-stack of 1 μm optical sections followed by adjusting the density, brightness and contrast. Although the gamma value was unadjusted for routine data processing, gamma values were adjusted from the standard value of 1.0 specifically for 3D rendering. Imaging data sets were exported to Adobe Photoshop CS2 where montages of representative data were generated.

Cell Counting of *Wnt1*-derived Purkinje Cells

Wnt1-derived Purkinje cells were manually counted on twelve adult sagittal sections from *Wnt1-CreER^T;mGFP* mice (n=3 across two litters for each fate mapping time point). The twelve sections were taken evenly across the full medial to lateral extent of the Cb and sequentially grouped into four categories: medial, medial-intermediate, lateral-intermediate, and lateral. The most lateral section from one fate mapped brain with marking at E13.5 was damaged and unable to be included in this analysis. Average cell counts per section were used to compare how *Wnt1* expressing progenitors from distinct developmental stages differentially contribute to the Purkinje cells.

Results

Wnt1 expressing progenitors in r1 have a diverse molecular identity

We initially evaluated *Wnt1* expression during Cb development by ISH. *Wnt1* was most prominently expressed in the URL between E11.5 and E12.5 (Fig. 1A,E,I,M, arrows), but was also observed at E10.5 and E13.5 (data not shown) consistent with previous reports (Wilkinson et al., 1987). By ISH, we demonstrated that *Wnt1* expression was largely complementary to *Math1* expression. Specifically, *Math1* expression was observed outside the URL in migrating progenitor cells while *Wnt1* expression was strictly confined to the URL. Within the URL, *Wnt1* overlapped slightly with *Math1* anteriorly, but *Wnt1* expression extended beyond the *Math1* expression domain to delineate the posterior URL (Fig. 1A–B,E–F,I–J,M–N). We used the *Wnt1-Venus* transgenic line (Brown et al., 2011) to better define the URL. First, we showed that *Wnt1-Venus* expression largely recapitulated endogenous *Wnt1* expression in r1 as shown by comparing ISH with labeled RNA probes for *Wnt1* and *GFP* on adjacent sections from age-matched wildtype and *Wnt1-Venus* littermates (Fig. S1). ICC with an anti-GFP antibody and biomarkers were then used on sections from *Wnt1-Venus* transgenic embryos to further characterize the molecular identity of *Wnt1* expressing progenitors in r1 (Fig. 1C–D,G–H,K–L,O–P). In particular, we used LMX1a as a marker for the posterior URL and roof plate and OTX2 to delineate the roof plate. At E11.5 and E12.5, a subset of *Wnt1* expressing cells expressed LMX1a at the most posterior limit of the URL (Fig. 1C,G,K,O, white arrows). *Wnt1* expression also extended into the roof plate where a WNT1+/LMX1a+/OTX2+ domain was observed (Fig. 1C–D,G–H,K–L,O–P, red arrows). In addition, *Wnt1* expressing progenitors were positioned anterior to the LMX1a and OTX2 expression domains (Fig. 1C–D,G–H,K–L,O–P, white arrowheads). Collectively, our biomarker analysis revealed molecularly distinct subpopulations of *Wnt1* expressing cells within the URL, which are listed from anterior to posterior, as follows: an anterior WNT1$^+$/MATH1$^+$/LMX1a$^-$/OTX2$^-$ zone, an intermediate WNT1$^+$/MATH1$^+$/LMX1a$^+$/OTX2$^-$, and a posterior WNT1$^+$/MATH1$^-$/LMX1a$^+$/OTX2$^-$ zone. Finally, the migratory stream in medial r1 did not contain any GFP$^+$ cells by ISH or by ICC (Fig. 1A–H) further validating that *Wnt1* expression is downregulated before Cb progenitors leave the germinal zone. In contrast, GFP$^+$ cells detected by ICC, but not *Wnt1* transcripts, were seen streaming away from the lateral URL at E11.5 and E12.5 (Fig. 1I–P, open arrowheads). The *Wnt1* and *GFP* transcripts were never observed in the migratory stream implicating some GFP protein perdurance (Fig. S1I,L). We exploited this GFP perdurance as a short term lineage tracer and showed that once lateral URL progenitors downregulated *Wnt1*, they rapidly migrated along the Cb surface. The perdurance of GFP also labeled *Wnt1* lineage cells that contributed to the choroid plexus.

The timing of *Wnt1* expression in URL progenitors predicts the spatial distribution of the Wnt1 lineage in the adult Cb

The spatial and temporal fate map of the *Wnt1* lineage in r1 has not been determined, but would resolve whether *Wnt1* expressing cells function merely as a transient signaling center in the URL or if they contribute to Cb cell types. Therefore, we utilized GIFM (reviewed in Joyner and Zervas, 2006; Dymecki and Kim, 2007) with *Wnt1-CreER^T* and conditional reporter mouse lines to permanently mark and track *Wnt1* expressing progenitors and their descendants (Zervas et al., 2004; Ellisor et al., 2009; Brown et al., 2011). For this current study, we first verified that the *Wnt1-CreER^T* transgene recapitulated endogenous *Wnt1* expression in r1 by comparing ISH with labeled RNA probes for *Wnt1* and *Cre* on adjacent sections (Fig. S2). Next, based on our characterization of *Wnt1* and *CreER^T* expression in r1 (Fig. 1,S2), we administered tamoxifen to *Wnt1-CreER^T;mGFP* embryos at E10.5, E11.5, E12.5, or E13.5 to specifically mark and track the *Wnt1* lineage derived from the URL.

During embryonic development, deep cerebellar neuron progenitors are the first cell type to emerge from the URL and therefore, we began our analysis by characterizing the *Wnt1* contribution to DCN (plane of sectioning shown in Fig. S3). *Wnt1* expressing progenitors in r1 marked at E10.5 gave rise to cells within all three DCN (Fig. 2A–C), but preferentially populated the intermediate and lateral DCN (the interpositus and dentate nuclei respectively). Few *Wnt1*-derived neurons were found within the medial fastigial nuclei. The fastigial nuclei primarily contained fate mapped cells with small nuclei (Fig. 2A, arrowhead) while the interpositus had larger fate mapped cells (Fig. 2B, arrow) and the dentate had a combination of both (Fig. 2C). *Wnt1* expressing progenitors marked at E11.5 resulted in the greatest contribution to the DCN and produced both large and small cell types across all three nuclei (Fig. 2D–F). In striking contrast to E10.5 marking, the *Wnt1* lineage marked at E12.5 primarily contributed to large neurons in the fastigial nuclei while the few *Wnt1*-derived cells in the more lateral DCN had smaller nuclei (Fig. 2G–I). Finally, late *Wnt1* expressing progenitors (marked from E13.5 onward) did not contribute to the DCN (data not shown). Thus, *Wnt1* expressing progenitors contributed to the DCN in a wave that began laterally at E10.5, peaked at E11.5 in all nuclei, and receded in a lateral to medial progression by E12.5. The size of *Wnt1*-derived DCN neurons also shifted with the extent of contribution.

The temporal contribution of the *Wnt1* lineage to granule cells and unipolar brush cells in the adult Cb

In contrast to early *Wnt1* expressing progenitors which substantially contributed to the DCN, the *Wnt1* lineage marked later in development predominantly gave rise to granule cells in the adult Cb cortex (Figs 3,4, plane of sectioning shown in Fig. S3). Tamoxifen administration and marking at E11.5 revealed that posterior folia VIII–X of the medial Cb (vermis) were heavily populated with *Wnt1*-derived granule neurons (Fig. 3A,D) while anterior folia I–V of the vermis had relatively fewer fate mapped cells (Fig. 3A,C). In contrast, *Wnt1*-derived granule neurons were evenly distributed across all folia in the Cb hemispheres when marked at E11.5 (Fig. 3B,E–F). Tamoxifen administration at E12.5 produced the peak of *Wnt1* contribution to granule neurons. *Wnt1*-derived granule neurons were located in all Cb folia with only a slight posterior bias at the midline (Fig. 4A,C,D). We bracketed these two major marking stages (E11.5 and E12.5) by fate mapping at E10.5 and E13.5 (Fig. 5). We observed only a small cohort of *Wnt1*-derived granule neurons in the most posterior vermis with marking at E10.5 (Fig. 5A), which increased with marking at E11.5 and E12.5 (Fig. 5B,C), and receded again at E13.5 (Fig. 5D). Thus, *Wnt1* expressing progenitors contributed to granule cells in a wave that arose at E10.5 with a medial posterior bias, peaked at E12.5, and diminished by E13.5.

Our GIFM experiments also uncovered *Wnt1*-derived cells within the granular layer of the posterior vermis that did not have the classic morphology of granule neurons. Since unipolar brush cells reside exclusively in this region (folia IX and X), we assessed these neurons for the expression of calretinin (CALR), a calcium binding protein expressed in a subpopulation of unipolar brush cells (Englund et al., 2006). The *Wnt1* lineage contributed moderately to CALR$^+$ unipolar brush cells with marking at E10.5, E11.5, and E13.5 (Fig. 5A,B,D) while marking at E12.5 produced the peak contribution (Fig. 5C). Thus, URL progenitors expressing *Wnt1* at E10.5 initiated the contribution to unipolar brush cells and the *Wnt1* lineage continued to give rise to unipolar brush cells until E13.5. At each marking stage, β-Gal$^+$/CALR$^-$ cells with relatively large nuclei were also seen in the granular layer. Based on their size, these cells were not granule cells and may represent another subpopulation of unipolar brush cells (CALR$^-$) (Englund et al., 2006). Alternatively, these cells may be inhibitory interneurons.

The *Wnt1* lineage and ventricular zone derivatives

Surprisingly, the *Wnt1* lineage also contributed to neurons within the Purkinje cell layer and molecular layer that are typically derived from the ventricular zone. We used cell-type specific biomarkers in conjunction with anti-β-gal antibodies to determine the cellular identity of these *Wnt1*-derivatives (Fig. 6). Specifically, *Wnt1*-derived Purkinje cells were identified by their distinct morphology and the expression of the calcium binding protein, calbindin (CALB, Fig. 6A–C). We took advantage of the sparsity and clarity of labeling and quantified the temporal contribution of the *Wnt1* lineage to Purkinje cells (Fig. S4). The *Wnt1* lineage produced very few Purkinje cells scattered throughout the entire Cb cortex when marked at marked at E9.5 and E10.5 (0.97 ± 2.02/section and 0.75 ± 1.00/section, respectively) (Fig. S4). A notable increase in *Wnt1*-derived Purkinje cells was observed by marking at E11.5 (6.89 ± 4.28/section). This wave of *Wnt1* contribution to Purkinje cells peaked with tamoxifen administration at E12.5 (16.08 ± 7.64/section) and declined with marking at E13.5 (6.89 ± 7.67/section). Purkinje cells derived from *Wnt1* expressing progenitors were evenly distributed in each folia across the medial to lateral extent of the adult Cb (Fig. S4). We also observed a general trend when marking at E11.5 and E12.5 whereby the *Wnt1* lineage contributed less to the medial versus intermediate and lateral Cb (Fig. S4). In an independent experiment using the *Z/EG* reporter (Novak et al., 2000), we identified *Wnt1*-derived cells located in close apposition to CALB$^+$ Purkinje cells (Fig. 6C,D) that were not seen with the neuron specific *mGFP* reporter line (Fig. 6A,B). Based on these observations and the cell morphology, we identified these *Wnt1*-derived cells as Bergmann glia. The neuron specific *mGFP* reporter also revealed sparse colabeling between the β-gal lineage tracer and inhibitory interneuron markers (PAX2 or Parvalbumin (PARV)) (Fig. 6E–F). Collectively, our biomarker analysis demonstrated that *Wnt1* expressing progenitors in r1 contribute to a small cohort of neurons and glia known to be derived from the Cb ventricular zone (Yamada and Watanabe, 2002; Carletti and Rossi, 2008).

Epochs of *Wnt1* expression guide the spatial distribution and molecular identity of the *Wnt1* lineage in the developing Cb

By conditionally deleting β-catenin in the *Wnt1* expression domain, a previous study clearly indicated that secreted WNT1 and the resultant WNT signaling cascade in the mes is vitally important for maintaining the isthmus organizer and patterning the Cb primordia (Brault et al., 2001). Our adult fate mapping results have demonstrated that *Wnt1* expressing cells within r1 do not merely constitute a transient signaling center, but rather are true progenitors that contribute to the Cb. These findings suggested that *Wnt1* expression within Cb progenitors might cell autonomously instruct the *Wnt1* lineage to exhibit specific cell behaviors during development. Therefore, we determined the developmental progression of the *Wnt1* lineage using GIFM to link transient *Wnt1* expression in r1 progenitors with cell migration, differentiation, and terminal cell fate. In these developmental fate mapping experiments, we used the *Rosa26^{tdTomato}* (Madisen et al., 2010) to trace the *Wnt1* lineage because the *mGFP* reporter line does not label neuronal progenitors at embryonic stages. We administered tamoxifen to *Wnt1-CreER^T;Rosa26^{tdTomato}* at E10.5, E11.5, E12.5, or E13.5 and analyzed the migratory progress and molecular identity of the *Wnt1* lineage at E14.5, E18.5 and P7. We observed that progenitors expressing *Wnt1* at specific embryonic stages differentially populate the embryonic and early postnatal Cb (Figs. 7–9).

In short term fate mapping experiments, the *Wnt1* lineage marked at E10.5 was located in the posterior URL (arrowheads), along the surface of the Cb primordia, and within the anterior extent of the intermediate and lateral Cb by E14.5 (Fig. 7A–C). In contrast, the *Wnt1* lineage marked at E12.5 was positioned throughout the anterior to posterior extent of the URL and more densely packed along the surface of the Cb primordia at E14.5 (Fig. 7D–F). In addition, progenitors with a history of *Wnt1* expression at E12.5 only sparsely

populate the anterior Cb (Fig. 7D–F). Interestingly, a few fate mapped cells were seen above the ventricular zone with marking at E12.5 and may be the source of the *Wnt1*-derived inhibitory interneurons (Fig. 7C–E, open arrowheads, insets).

Our intermediate stage lineage analysis showed that by late embryogenesis (E18.5) the *Wnt1* lineage marked at E10.5 gave rise to sporadically distributed cells located within the core of the developing Cb and very few cells in the medial URL (Fig. 8A; inset) and posterior external granular layer (EGL) (Fig. 8A, open arrowheads). Notably, no *Wnt1*-derived cells were found in the lateral URL or EGL at E18.5 (Fig. 8B; inset). With marking at E11.5, the *Wnt1* lineage had a similar spatial distribution when analyzed at E18.5 compared to marking a day earlier. However, the contribution to the Cb core, URL, and posterior EGL was greater (Fig. 8C,D). The *Wnt1* lineage marked at E12.5 generated cells in the Cb core at E18.5, but the contribution was diminished compared to marking a day earlier (Fig. 8E–F). At this marking stage, the *Wnt1* lineage contributed more substantially to the URL and EGL. Similarly, the *Wnt1* lineage marked at E13.5 still contributed to the URL and EGL with a posterior bias, but no longer gave rise to cells in the Cb core (Fig. 8G–H). Interestingly, the *Wnt1* lineage marked at E12.5 and more so at E13.5 began to delineate the initial sites of foliation at E18.5.

By P7, the *Wnt1* lineage marked at E10.5 sparsely populated the DCN, EGL, and internal granular layer (IGL) of the posterior vermis (Figs. 9A,S5A–C) whilst a more substantial contribution was observed in the EGL and IGL of the hemispheres (Fig. 9B). The *Wnt1*-derived contribution to the DCN and Cb cortex notably increased with marking at E11.5 (Figs. 9C–D,S5D–F). The *Wnt1* lineage substantially populated the posterior vermis, but was more sparsely and evenly distributed in the hemispheres (Fig. 9C–D). The *Wnt1* lineage marked at E12.5 generated cells in the DCN, but the contribution was diminished compared to marking a day earlier (Figs. 9E–F,S5G–I). With marking at E12.5, the *Wnt1* lineage contribution to the IGL and EGL was strikingly increased from previous fate mapping stages, but continued to exhibit a posterior bias medially, which was not detected laterally (Fig. 9E–F). Finally, the *Wnt1* lineage marked at E13.5 still contributed substantially to the IGL and EGL with a posterior bias but no longer gave rise to cells in the DCN at P7 (Fig. 9G–H).

As postnatal development proceeds, Cb precursors settle into their final location, differentiate, and acquire the molecular identity of mature Cb cell types. Therefore, we used a panel of cell-type specific biomarkers in conjunction with anti-DsRed ICC to confirm when *Wnt1* expressing progenitors acquired their mature molecular identity. (Fig. 10). As with our adult fate mapping experiments, we used CALR as a marker of unipolar brush cells (Englund et al., 2006), PAX2 as a marker for inhibitory interneurons of the granular layer, and PARV as a marker for Purkinje cells and inhibitory interneurons of the molecular layer. In our P7 analysis, we determined that *Wnt1* expressing progenitors substantially contributed to CALR[+] unipolar brush cells (Fig. 10A,B,E,F), but only sparsely gave rise to PAX2^{+} inhibitory interneurons (Fig. 10C,D,G,H), PARV^{+} Purkinje cells (Fig. 10I,J,M,N), and Bergmann glia (Fig. 10K,L,O,P). These results coincide with the molecular profile of the *Wnt1* lineage in the adult and indicate that *Wnt1* expressing progenitors differentiate in a time course that is typical for each Cb cell types.

The temporal dissection of the *Wnt1*-derived contribution to the precerebellar system

In our developmental analysis, prominent *Wnt1*-derived axonal projections from the inferior cerebellar peduncle were observed innervating the lateral Cb with marking at E10.5-E12.5 (Figs. 8,9, arrowheads, and S6). Based on these findings, we further examined how the timing of *Wnt1* expression in extra-cerebellar domains was related to the emergence of *Wnt1*-derived projections within the Cb. Analysis at E18.5 revealed that longitudinally

oriented projections entered the Cb laterally, turned perpendicularly, and coursed medially as evidenced by the round appearance of these fascicles in cross section (Figs. 8A–F,S6A–C). At P7, axonal projections from *Wnt1*-derived neurons marked at E10.5–E12.5 preferentially innervated the central vermis (folia VI–VIII) and lateral hemispheres (Figs. 9A–F,S6D–I). With marking at E13.5, axonal projections innervating the Cb were no longer derived from the *Wnt1* lineage (Figs. 8G–H,9G–H).

A group of six hindbrain nuclei known as the precerebellar system, provide the primary source of input to the Cb. Previous cumulative fate mapping studies demonstrated that *Wnt1* expressing progenitors in the LRL give rise to cells in the precerebellar system (Rodriguez and Dymecki, 2000; Zervas et al., 2004; Landsberg et al., 2005). With the temporal control of our GIFM system, we built upon this previous work and systematically determined how progenitors expressing *Wnt1* at particular developmental stages contribute to each precerebellar nucleus in the adult. *Wnt1* expressing progenitors marked at E8.5, E9.5, E10.5, E11.5, E12.5, or E13.5 gave rise to cells in each of the six precerebellar nuclei. Interestingly, the *Wnt1* contribution to each nuclei shifted substantially over the course of development (Fig. 11). Specifically, the greatest marking in the vestibular nuclei (VN) occurred with fate mapping at E9.5 (Fig. 11A,B) while peak marking in the lateral reticular nuclei (LRN) was produced by marking at E10.5 and E11.5 (Fig. 11I,J). The external cuneate nuclei (ECN), reticulotegmental nuclei (RTN), and pontine nuclei (PGN) received a more substantial and prolonged contribution from the *Wnt1* lineage with a peak from E10.5 to E13.5 (Fig. 11C,D,G,H,K,L). In contrast, the inferior olivary nuclei (ION) contained only a small population of fate mapped cells marked at E10.5 and E11.5 (Fig. 11E,F). Despite the temporal shift in the fate of *Wnt1* expressing progenitors, we did not observe any differences in the spatial distribution of *Wnt1*-derived cells within each nucleus.

Discussion

The dynamic nature of *Wnt1* expression in the Cb primordia obfuscates how progenitors expressing this gene contribute to the mature Cb. Therefore, we used GIFM to overcome this limitation. GIFM reveals that *Wnt1* expressing cells in the URL do not merely comprise a transient signaling center, but rather give rise to spatially and molecularly distinct Cb subpopulations at different embryonic stages. Through the study of other developmental systems, two primary models for cell fate determination have emerged: the progressive lineage restriction model and the competence model. In the progressive lineage restriction model, progenitors are initially able to give rise to all cell classes of a particular tissue, but as development proceeds, their potential becomes progressively limited to fewer and fewer cell types. Alternatively, in the competency model, progenitors pass through multiple waves of competence in which they are able to produce only a subset of cell types (Livesey and Cepko, 2001). Based on these criteria, the *Wnt1* lineage is not progressively restricted in its contribution to the Cb and a competency model more appropriately describes how *Wnt1* expressing progenitors generate the diverse array of Cb cell types. Moreover, the distinct rise, peak, and fall of marking across different temporal windows indicates that *Wnt1* expression is induced *de novo* in the URL as development progresses. Specifically, early *Wnt1* expressing progenitors in r1 primarily contribute to the DCN (E10.5–E12.5) while later *Wnt1* expressing progenitors shift to a predominantly granule cell fate (E11.5–E13.5). The contribution of the *Wnt1* lineage corresponds well with the migratory profile of these two cell types. For example, at E12.5, granule cell progenitors are just starting to emerge from the URL while DCN progenitors have already completed their migration away from the germinal zone (Fink et al., 2006; Carletti and Rossi, 2008). In contrast, *Wnt1* expressing progenitors allocated toward a unipolar brush cell fate express *Wnt1* well before these cells migrate away from the URL during late embryogenesis (Englund et al., 2006). These results suggest that *Wnt1*-derived unipolar brush cell progenitors express *Wnt1* relatively early in

their cellular development (E10.5-E13.5) and subsequently extinguish *Wnt1* expression long before they emerge from the URL. Interestingly, our developmental analysis revealed that early *Wnt1* expressing progenitors also ir migration from the URL while later *Wnt1* expressing progenitors transition away from the germinal zone. For example, the first granule cells to emerge from the URL normally populate the anterior EGL/IGL while granule cells migrating away from the URL later in embryogenesis fill in behind to inhabit the posterior EGL/IGL (Altman and Bayer, 1997). However, granule cell precursors derived from the *Wnt1* lineage marked at E11.5 remain relatively confined to the posterior-most EGL while the *Wnt1* lineage marked at E13.5 extends into the anterior EGL at E18.5 and P7. Based on these results, the induction and termination of *Wnt1* expression does not regulate when the *Wnt1* lineage emerges from the URL. Rather, early *Wnt1* expression may be linked to early granule cell differentiation. For example, granule cells derived from the *Wnt1* lineage marked at E10.5 and E11.5 are predominantly located in the differentiated EGL by P7 while *Wnt1*-derived granule cells marked at E12.5 and E13.5 are distributed in both the differentiated EGL and undifferentiated IGL.

Our GIFM experiments reveal a spatial bias of *Wnt1* lineage contribution to the Cb. For example, *Wnt1*-derived neurons populate the lateral DCN before the medial DCN. In contrast, *Wnt1*-derived granule neurons marked across all time points preferentially reside in the posterior vermis. Interestingly, this posterior bias is not be observed laterally, possibly because the sparsely labeled anterior lobe (lobules I–V) is not contiguous with the Cb hemispheres (Altman and Bayer, 1997). These spatial biases may also reflect the distinct morphogenic movements that establish the location of cell types within the mature Cb. In particular, some granule cells from the lateral URL migrate medially during postnatal development to populate the posterior folia of the vermis (Sgaier et al., 2005). Therefore, the preponderance of *Wnt1*-derived granule cells in the posterior folia of the medial Cb may be a consequence of this medial migration. Moreover, the spatial differences could indicate a role for *Wnt1* in a combinatorial and temporally regulated genetic code that determines cell fate within the URL.

Currently, the URL and ventricular zone are viewed as separate Cb germinal zones that broadly compartmentalize neurogenesis into excitatory and inhibitory progenitor populations (Hoshino et al., 2005; Machold and Fishell, 2005; Wang et al., 2005). Surprisingly, *Wnt1* expressing progenitors produce ventricular zone derivatives including inhibitory interneurons and Bergmann glia. Small cohorts of *Wnt1*-derived inhibitory interneurons are observed at each fate mapping stage and *Wnt1* expressing progenitors contribute to Purkinje cells in a distinct temporal wave. If neurogenesis is truly segregated into two germinal zones, our results suggest that cells with a history of *Wnt1* expression may extend from the URL into the posterior limit of the ventricular zone. In this regard, *Wnt1* expression is primarily restricted to the URL but a promiscuous interface between the URL and ventricular zone allows some cells at the interface to enter the adjacent domain. Our short term fate mapping analysis identified sparse *Wnt1*-derived cells near the ventricular zone at E14.5, which may serve as the source for our *Wnt1*-derived inhibitory interneurons. Alternatively, faint expression of *CreER^T* beyond the URL in some sections from our *Wnt1-CreER^T* transgenic line could account for the ventricular zone derivatives observed in this fate mapping study (Fig S2). However, this explanation is unlikely because *CreER^T in situ* labeling outside the URL is similar to background levels. More importantly, our *Wnt1* fate mapping results are supported by earlier studies using β-gal perdurance in *Wnt1-LacZ* transgenic mice (Nichols and Bruce, 2006) and GFP perdurance in *wnt1-GVP-UG* transgenic zebrafish (Volkmann et al., 2010) to transiently follow progenitors with a history of *Wnt1* expression. Furthermore, *Wnt1* has a comparable expression domain to *Wnt3a* in the URL and the *Wnt3a* lineage gives rise to similar Cb cell types as the *Wnt1* lineage (Louvi et al., 2007). Therefore, the most parsimonious explanation for our results is

that the interface between the URL and the ventricular zone is not a rigid partition and although the *Wnt1* lineage produces some ventricular zone derivatives, *Wnt1* expressing progenitors primarily contribute to the DCN, granule cells, and unipolar brush cells.

Within each germinal zone, Cb progenitors are subdivided based on their molecular identity (Morales and Hatten, 2006; Zordan et al., 2008; Liu et al., 2010). Our characterization of *Wnt1* expression in URL demonstrates an increasingly complex molecular heterogeneity in this dynamic germinal zone. Previous studies describing *Math1* and *Lmx1a* expression in the URL showed that the posterior limit of *Math1* intermingles with the *Lmx1a* expression domain (Akazawa et al., 1995; Chizhikov et al., 2010). Our findings show that *Wnt1* expression bridges the *Otx2*, *Lmx1a,* and *Math1* domains. Therefore, *Wnt1* expressing progenitors in URL can be partitioned into three molecularly distinct rostral to caudal zones: 1. WNT1$^+$/MATH1$^+$/LMX1a$^-$, 2. WNT1$^+$/MATH1$^+$/LMX1a$^+$, and 3. WNT1$^+$/MATH1$^-$/LMX1a$^+$. By integrating our *Wnt1* GIFM results with *Math1* and *Lmx1a* fate mapping, we can construct a basic model for how combinatorial gene expression patterns in the URL are translated into cell fate during development. Both *Wnt1* and *Math1* fate mapping experiments reveal that DCN neurons are derived from marking at E10.5-E12.5 (Machold and Fishell, 2005). In contrast, the *Lmx1a* lineage does not produce DCN neurons (Chizhikov et al., 2010). Therefore, a cohort of DCN progenitors are *Wnt1$^+$/Math1$^+$/Lmx1a$^-$*, consistent with URL zone 1. Granule cells are differentially derived from the *Wnt1* lineage (marking at E10.5-E13.5) versus *Math1* lineage (marking at E12.5 through postnatal stages) (Machold and Fishell, 2005). The *Lmx1a* lineage also gives rise to granule cells (Chizhikov et al., 2010). These findings suggest that *Wnt1* expressing progenitors migrate from URL zone 3 to zone 1 coincident with the upregulation of *Math1* and subsequent downregulation of *Lmx1a*. This transition is consistent with the role of *Math1* in initiating the migration of progenitors away from the URL (Machold and Fishell, 2005) and the proposed role of *Lmx1a* in repressing *Math1* expression to prevent premature migration of URL progenitors (Chizhikov et al., 2010).

The precise molecular interactions between LMX1a, WNT1 and MATH1 in the URL remain unresolved. However, *Wnt1$^{-/-}$* mutants display decreased *Math1* expression in the LRL (Ikeya et al., 1997). Moreover, β-catenin, a downstream component of canonical WNT signaling, binds to the *Math1* enhancer and promotes *Math1* expression (Shi et al., 2010). These findings suggest that *Wnt1* signaling promotes *Math1* expression in the URL. To test whether β-catenin is active in the URL, we assessed embryos expressing *TOPGAL*, a reporter for canonical WNT signaling (DasGupta and Fuchs, 1999). We rarely detected WNT responding cells in the URL although responsive cells were detected in other locations (Fig. S7, data not shown). Therefore, *Wnt1* may act through non-canonical pathways (Spinsanti et al., 2008) to regulate *Math1* expression in the URL. Alternatively, canonical WNT signaling in the URL might be below the particular threshold required for detection by the TOPGAL reporter. Finally, *Wnt1* expression is downregulated before Cb progenitors migrate away from URL zone 3 suggesting that WNT1 is not required for the continued maintenance of *Math1* expression outside of the URL.

Cumulative and intersectional fate mapping approaches have spatially dissected the LRL and linked molecularly distinct progenitor domains to cell fate in the precerebellar system (Rodriguez and Dymecki, 2000; Landsberg et al., 2005; Wang et al., 2005; Yamada and Watanabe, 2002; Ray and Dymecki, 2009). Moreover, previous work determined that *Wnt1* expressing progenitors contribute to the precerebellar nuclei (Zervas et al., 2004; Landsberg et al., 2005). Our GIFM study expands upon those results by providing detailed temporal resolution to the *Wnt1* fate map in the precerebellar system. We found that the marking stages that generated the peak *Wnt1* contribution to each precerebellar nuclei correspond to the birthdate of that particular nucleus (Altman and Bayer, 1997). In addition, the *Wnt1*

lineage gives rise to the precerebellar system at the same developmental stages in which *Wnt1* expressing progenitors in the URL establish the cytoarchitecture of the Cb. Finally, *Wnt1*-derived axonal projections from the precerebellar system innervate regions populated by Cb descendants of the *Wnt1* lineage. Perhaps *Wnt1* expression facilitates a molecular matching between the precerebellar nuclei with their Cb targets. In this regard, the spatial and temporal regulation of *Wnt1* has the potential to form an entirely *Wnt1* derived neural circuit in the Cb.

Conclusions

In summary, this study successfully used a novel transgenic reporter allele, *Wnt1-Venus,* to molecularly dissect the URL and uncovered three molecularly distinct developmental zones based on the expression of *Wnt1*, *Math1*, and *Lmx1a.* By fate mapping the *Wnt1* lineage, we determined that *Wnt1* expressing cells in the URL are not merely a transient signaling center, but serve as true Cb progenitors. In particular, the *Wnt1* lineage gives rise to many excitatory Cb cell types as well as sparse inhibitory neurons and Bergmann glia. More importantly, the temporal dissection of the *Wnt1* lineage revealed that *Wnt1* expressing progenitors produce each Cb cell type in a distinct wave of contribution demonstrating that *Wnt1* expression is induced *de novo* in URL progenitors. In general, the temporal fate map of the *Wnt1* lineage in both the Cb and precerebellar system corresponded well with the birth order of each cell type. However, within each Cb cell class, early *Wnt1* expression did not necessarily translate into early migration from the URL. In this regard, *Wnt1* expressing cells are a valuable progenitor pool for the Cb and precerebellar system, but the specific role for *Wnt1* in the rhombic lip remains unknown.

Supplementary Material

Refer to Web version on PubMed Central for supplementary material.

Acknowledgments

References

Akazawa C, Ishibashi M, Shimizu C, Nakanishi S, Kageyama R. A mammalian helix-loop-helix factor structurally related to the product of Drosophila proneural gene atonal is a positive transcriptional regulator expressed in the developing nervous system. J Biol Chem. 1995; 270:8730–8738. [PubMed: 7721778]

Altman, J.; Bayer, S. Development of the cerebellar system in relation to its evolution, structure, and function. CRC Press; Boca Raton, FL: 1997.

Bally-Cuif L, Cholley B, Wassef M. Involvement of Wnt-1 in the formation of the mes/metencephalic boundary. Mech Dev. 1995; 53:23–34. [PubMed: 8555108]

Brault V, Moore R, Kutsch S, Ishibashi M, Rowitch DH, McMahon AP, Sommer L, Boussadia O, Kemler R. Inactivation of the beta-catenin gene by Wnt1-Cre-mediated deletion results in dramatic brain malformation and failure of craniofacial development. Development. 2001; 128:1253–1264. [PubMed: 11262227]

Brown A, Brown S, Ellisor D, Hagan N, Normand E, Zervas M. A Practical Approach to Genetic Inducible Fate Mapping: A Visual Guide to Mark and Track Cells *In Vivo.* J Vis Exp. 2009; 43:1687. pii. 10.3791/1687 [PubMed: 20042997]

Brown A, Machan JT, Zervas M. Molecular organization and timing of *Wnt1* expression define cohorts of midbrain dopamine neuron progenitors *in vivo*. J Comp Neurol. 2011; 519:2978–3000. [PubMed: 21713770]

Carletti B, Rossi F. Neurogenesis in the cerebellum. Neuroscientist. 2008; 14:91–100. [PubMed: 17911211]

Chizhikov VV, Lindgren AG, Mishima Y, Roberts RW, Aldinger KA, Miesegaes GR, Currle DS, Monuki ES, Millen KJ. Lmx1a regulates fates and location of cells originating from the cerebellar rhombic lip and telencephalic cortical hem. Proc Natl Acad Sci U S A. 2010; 107:10725–10730. [PubMed: 20498066]

Danielian PS, McMahon AP. Engrailed-1 as a target of the Wnt-1 signalling pathway in vertebrate midbrain development. Nature. 1996; 383:332–334. [PubMed: 8848044]

DasGupta R, Fuchs E. Multiple roles for activated LEF/TCF transcription complexes during hair follicle development and differentiation. Development. 1999; 126:4557–4568. [PubMed: 10498690]

Dymecki SM, Kim JC. Molecular neuroanatomy's "Three Gs": a primer. Neuron. 2007; 54:17–34. [PubMed: 17408575]

Ellisor D, Koveal D, Hagan N, Brown A, Zervas M. Comparative analysis of conditional reporter alleles in the developing embryo and embryonic nervous system. Gene Expr Patterns. 2009; 9:475–489. [PubMed: 19616131]

Ellisor D, Zervas M. Tamoxifen dose response and conditional cell marking: is there control? Mol Cell Neurosci. 2010; 45:132–138. [PubMed: 20600933]

Englund C, Kowalczyk T, Daza RA, Dagan A, Lau C, Rose MF, Hevner RF. Unipolar brush cells of the cerebellum are produced in the rhombic lip and migrate through developing white matter. J Neurosci. 2006; 26:9184–9195. [PubMed: 16957075]

Fink AJ, Englund C, Daza RA, Pham D, Lau C, Nivison M, Kowalczyk T, Hevner RF. Development of the deep cerebellar nuclei: transcription factors and cell migration from the rhombic lip. J Neurosci. 2006; 26:3066–3076. [PubMed: 16540585]

Guo Q, Loomis C, Joyner AL. Fate map of mouse ventral limb ectoderm and the apical ectodermal ridge. Dev Biol. 2003; 264:166–178. [PubMed: 14623239]

Hippenmeyer S, Vrieseling E, Sigrist M, Portmann T, Laengle C, Ladle DR, Arber S. A developmental switch in the response of DRG neurons to ETS transcription factor signaling. PLoS Biol. 2005; 3:e159. [PubMed: 15836427]

Hoshino M, Nakamura S, Mori K, Kawauchi T, Terao M, Nishimura YV, Fukuda A, Fuse T, Matsuo N, Sone M, Watanabe M, Bito H, Terashima T, Wright CV, Kawaguchi Y, Nakao K, Nabeshima Y. Ptf1a, a bHLH transcriptional gene, defines GABAergic neuronal fates in cerebellum. Neuron. 2005; 47:201–213. [PubMed: 16039563]

Ikeya M, Lee SM, Johnson JE, McMahon AP, Takada S. Wnt signalling required for expansion of neural crest and CNS progenitors. Nature. 1997; 389:966–970. [PubMed: 9353119]

Joyner AL, Zervas M. Genetic inducible fate mapping in mouse: establishing genetic lineages and defining genetic neuroanatomy in the nervous system. Dev Dyn. 2006; 235:2376–2385. [PubMed: 16871622]

Kimmel RA, Turnbull DH, Blanquet V, Wurst W, Loomis CA, Joyner AL. Two lineage boundaries coordinate vertebrate apical ectodermal ridge formation. Genes Dev. 2000; 14:1377–1389. [PubMed: 10837030]

Landsberg RL, Awatramani RB, Hunter NL, Farago AF, DiPietrantonio HJ, Rodriguez CI, Dymecki SM. Hindbrain rhombic lip is comprised of discrete progenitor cell populations allocated by Pax6. Neuron. 2005; 48:933–947. [PubMed: 16364898]

Liu A, Joyner AL. Early anterior/posterior patterning of the midbrain and cerebellum. Annu Rev Neurosci. 2001; 24:869–896. [PubMed: 11520921]

Liu ZR, Shi M, Hu ZL, Zheng MH, Du F, Zhao G, Ding YQ. A refined map of early gene expression in the dorsal rhombomere 1 of mouse embryos. Brain Res Bull. 2010; 82:74–82. [PubMed: 20206242]

Livesey FJ, Cepko CL. Vertebrate neural cell-fate determination: lessons from the retina. Nat Rev Neurosci. 2001; 2:109–118. [PubMed: 11252990]

Louvi A, Yoshida M, Grove EA. The derivatives of the Wnt3a lineage in the central nervous system. J Comp Neurol. 2007; 504:550–569. [PubMed: 17701978]

Machold R, Fishell G. Math1 is expressed in temporally discrete pools of cerebellar rhombic-lip neural progenitors. Neuron. 2005; 48:17–24. [PubMed: 16202705]

Madisen L, Zwingman TA, Sunkin SM, Oh SW, Zariwala HA, Gu H, Ng LL, Palmiter RD, Hawrylycz MJ, Jones AR, Lein ES, Zeng H. A robust and high-throughput Cre reporting and characterization system for the whole mouse brain. Nat Neurosci. 2010; 13:133–140. [PubMed: 20023653]

McMahon AP, Bradley A. The Wnt-1 (int-1) proto-oncogene is required for development of a large region of the mouse brain. Cell. 1990; 62:1073–1085. [PubMed: 2205396]

McMahon AP, Joyner AL, Bradley A, McMahon JA. The midbrain-hindbrain phenotype of Wnt-1-/ Wnt-1- mice results from stepwise deletion of engrailed-expressing cells by 9.5 days postcoitum. Cell. 1992; 69:581–595. [PubMed: 1534034]

Morales D, Hatten ME. Molecular markers of neuronal progenitors in the embryonic cerebellar anlage. J Neurosci. 2006; 26:12226–12236. [PubMed: 17122047]

Nichols DH, Bruce LL. Migratory routes and fates of cells transcribing the Wnt-1 gene in the murine hindbrain. Dev Dyn. 2006; 235:285–300. [PubMed: 16273520]

Novak A, Guo C, Yang W, Nagy A, Lobe CG. Z/EG, a double reporter mouse line that expresses enhanced green fluorescent protein upon Cre-mediated excision. Genesis. 2000; 28:147–155. [PubMed: 11105057]

Ray RS, Dymecki SM. Rautenlippe Redux -- toward a unified view of the precerebellar rhombic lip. Curr Opin Cell Biol. 2009; 21:741–747. [PubMed: 19883998]

Rodriguez CI, Dymecki SM. Origin of the precerebellar system. Neuron. 2000; 27:475–486. [PubMed: 11055431]

Sgaier SK, Millet S, Villanueva MP, Berenshteyn F, Song C, Joyner AL. Morphogenetic and cellular movements that shape the mouse cerebellum; insights from genetic fate mapping. Neuron. 2005; 45:27–40. [PubMed: 15629700]

Shi F, Cheng YF, Wang XL, Edge AS. Beta-catenin up-regulates Atoh1 expression in neural progenitor cells by interaction with an Atoh1 3′ enhancer. J Biol Chem. 2010; 285:392–400. [PubMed: 19864427]

Spinsanti P, De Vita T, Caruso A, Melchiorri D, Misasi R, Caricasole A, Nicoletti F. Differential activation of the calcium/protein kinase C and the canonical beta-catenin pathway by Wnt1 and Wnt7a produces opposite effects on cell proliferation in PC12 cells. J Neurochem. 2008; 104:1588–1598. [PubMed: 17988238]

Sunmonu NA, Li K, Guo Q, Li JY. Gbx2 and Fgf8 are sequentially required for formation of the midbrain-hindbrain compartment boundary. Development. 2011; 138:725–34. [PubMed: 21266408]

Thomas KR, Musci TS, Neumann PE, Capecchi MR. Swaying is a mutant allele of the proto-oncogene Wnt-1. Cell. 1991; 67:969–976. [PubMed: 1835670]

Volkmann K, Chen YY, Harris MP, Wullimann MF, Köster RW. The zebrafish cerebellar upper rhombic lip generates tegmental hindbrain nuclei by long-distance migration in an evolutionary conserved manner. J Comp Neurol. 2010; 518:2794–2817. [PubMed: 20506476]

Wang VY, Rose MF, Zoghbi HY. Math1 expression redefines the rhombic lip derivatives and reveals novel lineages within the brainstem and cerebellum. Neuron. 2005; 48:31–43. [PubMed: 16202707]

Wilkinson DG, Bailes JA, McMahon AP. Expression of the proto-oncogene int-1 is restricted to specific neural cells in the developing mouse embryo. Cell. 1987; 50:79–88. [PubMed: 3594565]

Yamada K, Watanabe M. Cytodifferentiation of Bergmann glia and its relationship with Purkinje cells. Anat Sci Int. 2002; 77:94–108. [PubMed: 12418089]

Zervas M, Millet S, Ahn S, Joyner AL. Cell behaviors and genetic lineages of the mesencephalon and rhombomere 1. Neuron. 2004; 43:345–357. [PubMed: 15294143]

Zordan P, Croci L, Hawkes R, Consalez GG. Comparative analysis of proneural gene expression in the embryonic cerebellum. Dev Dyn. 2008; 237:1726–1735. [PubMed: 18498101]
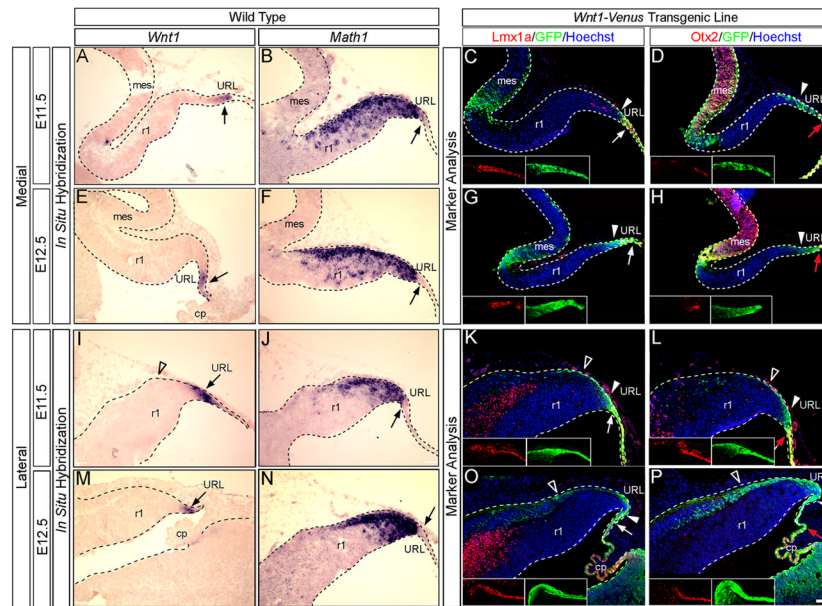
Fig. 1. *Wnt1* expression in r1
(A–B,E–F,I–J,M–N) ISH revealed *Wnt1* and *Math1* expression in the URL (arrow) in wild type mice at E11.5 and E12.5. **(C–D,G–H,K–L,O–P)** ICC with an anti-GFP antibody and indicated biomarkers on sections from *Wnt1-Venus* embryos uncovered a population of *Wnt1* expressing progenitors (green) coexpressing LMX1a (C,G,K,O red) in the posterior URL (white arrow) and OTX2 (D,H,L,P red) in the roof plate (red arrow). *Wnt1* expressing progenitors in the anterior URL did not express either of these markers (solid arrowhead). GFP perdurance was used as a transient lineage tracer and reveals *Wnt1*-derived cells in the lateral migratory stream (open arrowheads). Scale bar: 61 μm.
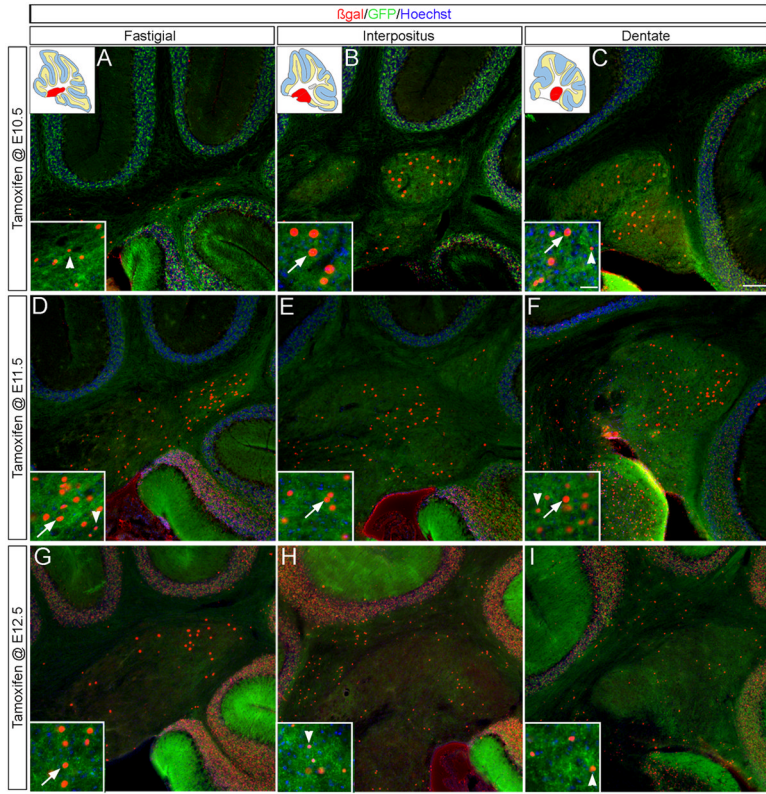
Fig. 2. *Wnt1* expressing progenitors temporally contributed to the DCN
ICC on adult sagittal sections with antibodies that recognized β-gal (red) or GFP (green)
revealed that *Wnt1* expressing progenitors contributed to all three DCN. **(A–C)** The *Wnt1*
lineage marked at E10.5 preferentially populated the interpositus and dentate nuclei. The
Wnt1-derived cells in these two nuclei have larger cell nuclei (arrows) than those in the
fastigial nuclei (arrowheads). **(D–F)** The *Wnt1* lineage marked at E11.5 represented the peak
of DCN marking. Cells with both large (arrows) and small (arrowheads) nuclei are found
across all three DCN. **(G–I)** The *Wnt1* lineage marked at E12.5 preferentially populated the
fastigial nuclei while the interpositus and dentate had fewer *Wnt1*-derived cells. The *Wnt1*-
derived cells in the fastigial nuclei had large cell nuclei (arrows) while those in the lateral
DCN had small nuclei (arrowheads). Scale bars: 120 μm (**A–I**), 30 μm (insets).
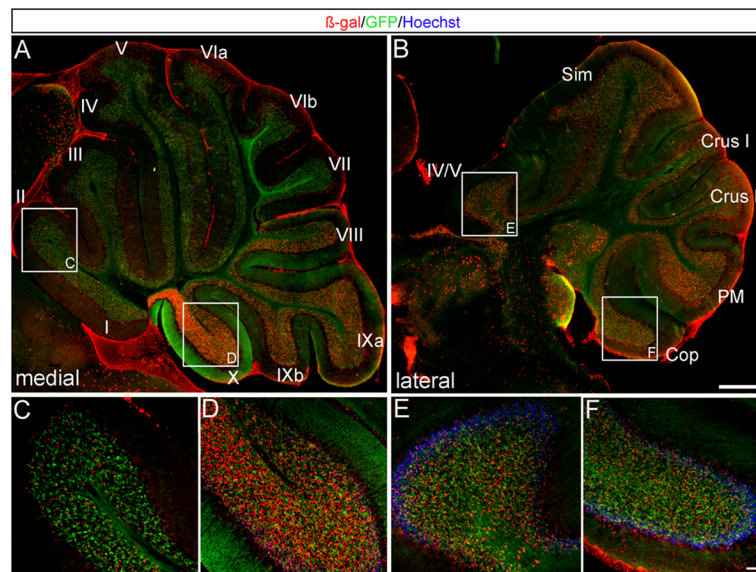
Fig. 3. The *Wnt1* lineage marked at E11.5 primarily contributed to the medial-posterior Cb cortex

ICC on adult sagittal sections with antibodies against β-gal (red) or GFP (green) revealed that *Wnt1* expressing cells at E11.5 gave rise to cells in the granular layer. (**A,C,D**) Medially, *Wnt1*-derived cells populated every folia, but a substantially greater contribution was seen in folia IX and X. (**B,E,F**) Laterally, fate mapped cells were evenly distributed across all folia and were less densely populated in the posterior Cb. Scale bars: 1.0 mm (**A,B**) 61 μm (**C–F**).
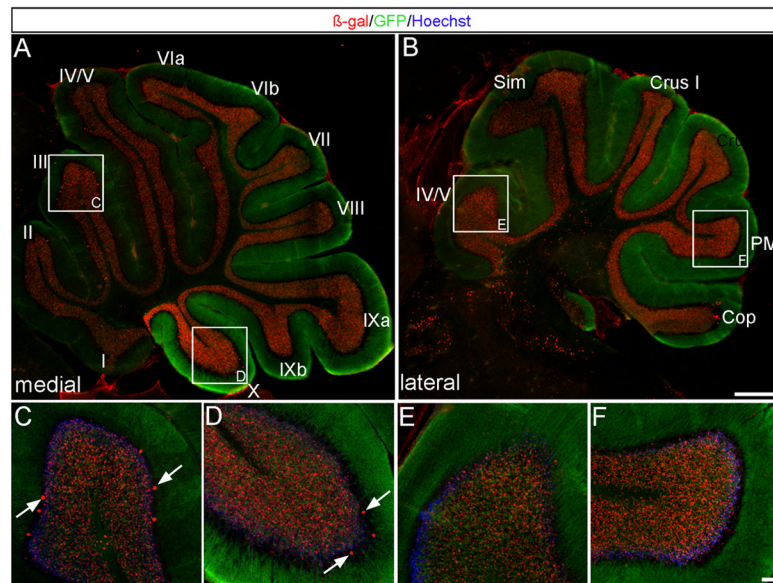
Fig. 4. The *Wnt1* lineage marked at E12.5 contributed to the entire Cb cortex
(A–F) ICC on adult sagittal sections with antibodies against β-gal (red) or GFP (green) revealed that *Wnt1* expressing cells at E12.5 populated the granular layer of every folia and represented the peak contribution to this region. *Wnt1*-derived Purkinje cells were also observed (C,D arrows). Scale bars: 1.0 mm (**A,B**) 61 μm (**C–F**).
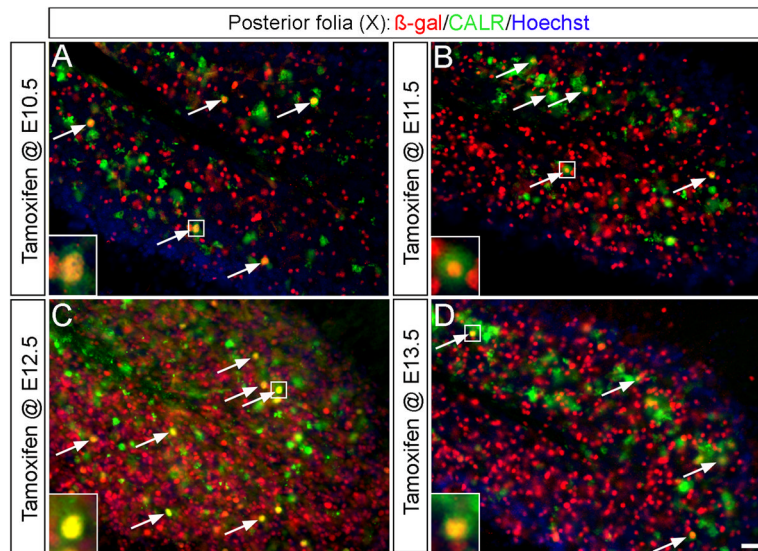
Fig. 5. Unipolar brush cells are derived from the *Wnt1* lineage
(A–D) ICC on adult sagittal sections with antibodies against β-gal (red) or Calretinin (CALR, green) uncovered that *Wnt1* expressing progenitor cells (red) contributed to unipolar brush cells (green) in the granular layer of folia IX and X (arrows). The *Wnt1* lineage from E12.5 **(C)** made the most substantial contribution. Scale bar: 30 μm.
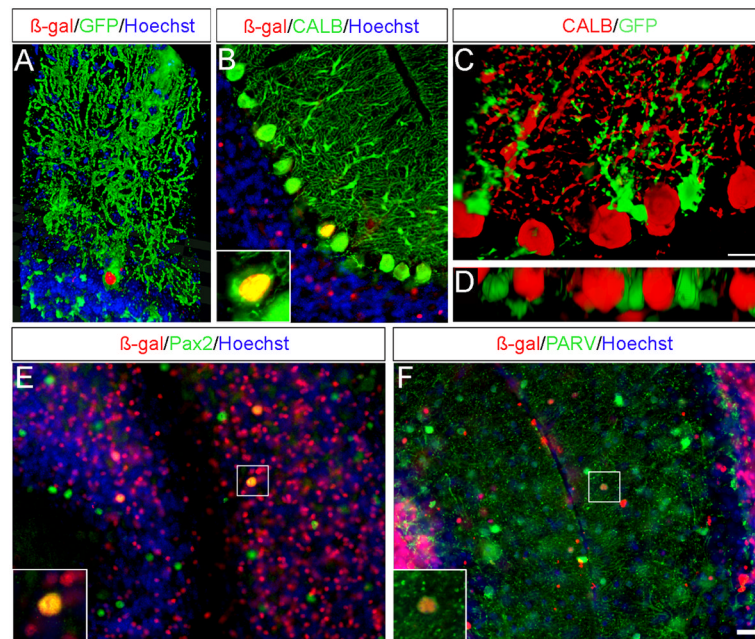
Fig. 6. Molecular analysis of the *Wnt1* lineage in the adult Cb cortex
ICC on adult sagittal sections with antibodies recognizing either β-gal or EGFP and cell type specific biomarkers. **(A)** Three dimensional rendering of a *Wnt1*-derived neuron marked at E11.5 (using the *mGFP* reporter) demonstrated the distinct morphology of a Purkinje cell with both nuclear β-gal (red) and membrane bound GFP (green) immunolabeling. **(B)** The contribution of the *Wnt1* lineage to scattered Purkinje cells was confirmed by Calbindin (CALB, green) labeling. **(C)** *Wnt1* fate mapping with the *Z/EG* reporter revealed that the *Wnt1* lineage (green) marked at E11.5 also contributed to Bergmann glia, identified based on their cell morphology and position between Purkinje cells (CALB, red). **(D)** Three dimensional rendering of the *Wnt1*-derived Bergmann glia viewed in the XZ plane showed their close apposition with Purkinje cells. **(E–F)** Antibody labeling against PAX2 (E, green) or PARV (F, green) showed that the *Wnt1* lineage marked at E12.5 contributed to a small population of inhibitory interneurons of the granular layer and molecular layer. Scale bar: 30 μm.
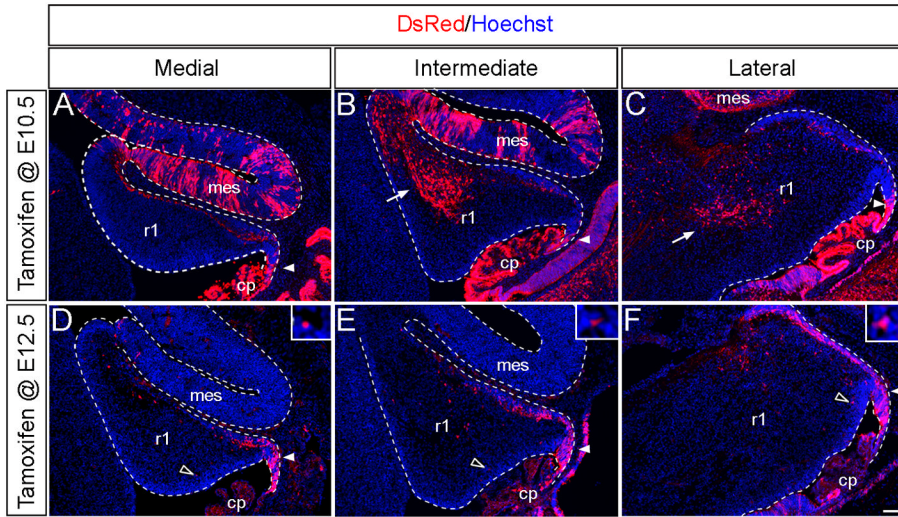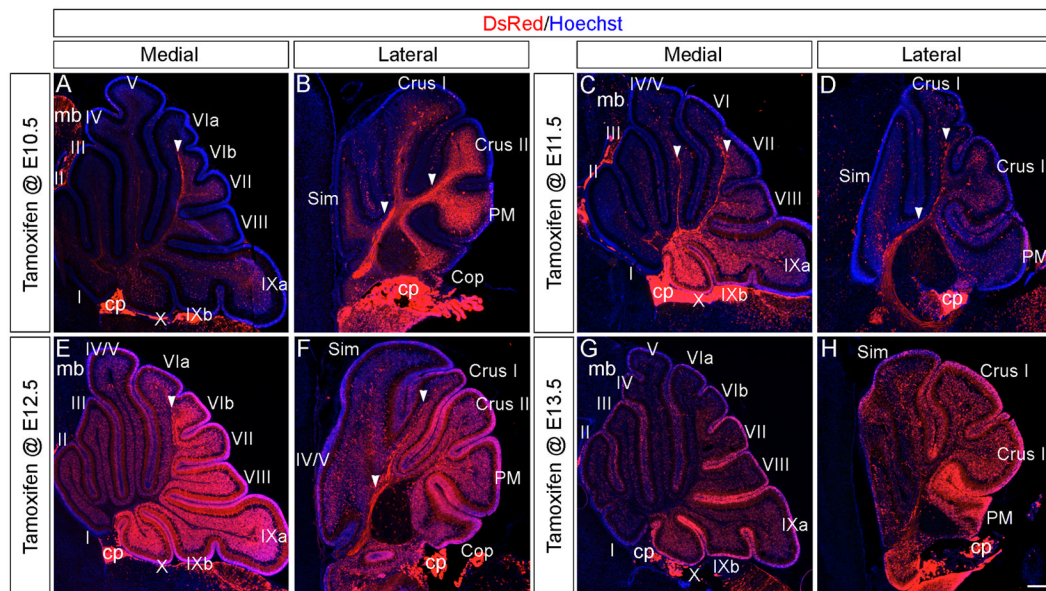
Fig. 7. *Wnt1* expressing progenitors
ICC with an antibody against tdTomato (DsRed, red) to detect the *Wnt1* lineage marked at
the indicated stages and analyzed on E14.5 sagittal sections. **(A,B,C)** The *Wnt1* lineage
marked at E10.5 was located in the posterior URL (arrowheads), along the surface of the Cb
primordia, and within the anterior extent of the intermediate (B) and lateral (C) Cb (arrows).
(C,D,E) The *Wnt1* lineage marked at E12.5 was positioned throughout the URL
(arrowheads) and along the surface of the Cb primordia. However, progenitors expressing
Wnt1 at E12.5 did not populate the anterior Cb. In addition, a few fate mapped cells were
seen above the ventricular zone with marking at E12.5 (open arrowheads). choroid plexus
(cp), midbrain (mb). Scale bar: 120 μm.
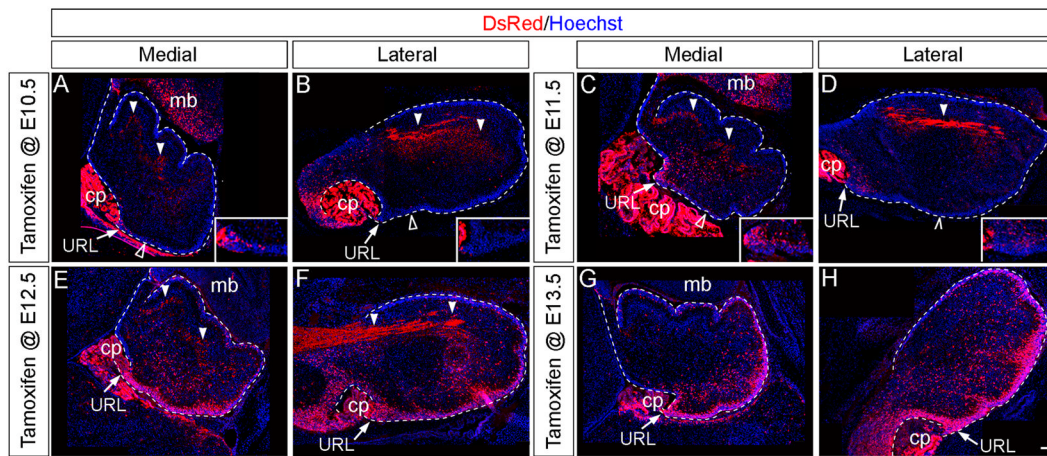
Fig. 8. ***Wnt1* expressing progenitors differentially migrate away from the URL by E18.5**
ICC with an antibody against tdTomato (DsRed, red) to detect the *Wnt1* lineage marked at the indicated stages and analyzed on E18.5 sagittal sections. **(A,B)** The *Wnt1* lineage marked at E10.5 was sparsely scattered within the Cb core, anterior URL (arrows, inset shows higher magnification of the URL), and posterior EGL (open arrowheads). *Wnt1*-derived projections (arrowheads) ran longitudinally in the lateral Cb and transversely in the medial Cb (projections are shown in more detail in Figure S6). **(C,D)** The *Wnt1* lineage marked at E11.5 had a similar distribution, but the extent of labeling was increased versus marking at E10.5. **(E,F)** The *Wnt1* lineage marked at E12.5 constituted the peak of Cb marking and produced an abundance of labeled cells within the URL, Cb core, and EGL at E18.5. **(G,H)** The *Wnt1* lineage marked at E13.5 contributed substantially to the EGL with a posterior bias. choroid plexus (cp), midbrain (mb). Scale bar: 120 μm.

Fig. 9. *Wnt1* expressing progenitors distinctively contributed to the developing Cb at P7
ICC with an antibody against tdTomato (DsRed, red) on P7 fate mapped sagittal sections.
(A,B) The *Wnt1* lineage marked at E10.5 primarily contributed to the Cb core, posterior
EGL, and posterior IGL. *Wnt1*-derived projections (arrowheads) were preferentially located
in folia VI–VII and the hemispheres at P7 **(C,D)** The *Wnt1* lineage marked at E11.5 had a
similar distribution, but the extent of labeling was increased from marking at E10.5. *Wnt1*-
derived cells populated every folia, but a greater contribution was seen in the posterior
vermis. **(E,F)** The *Wnt1* lineage from E12.5 constituted the peak of Cb marking and
produced cells within the DCN and Cb cortex. **(G,H)** The *Wnt1* lineage marked at E13.5
contributed substantially to the EGL and Cb cortex with a posterior bias. choroid plexus
(cp), midbrain (mb). Scale bar: 250 μm
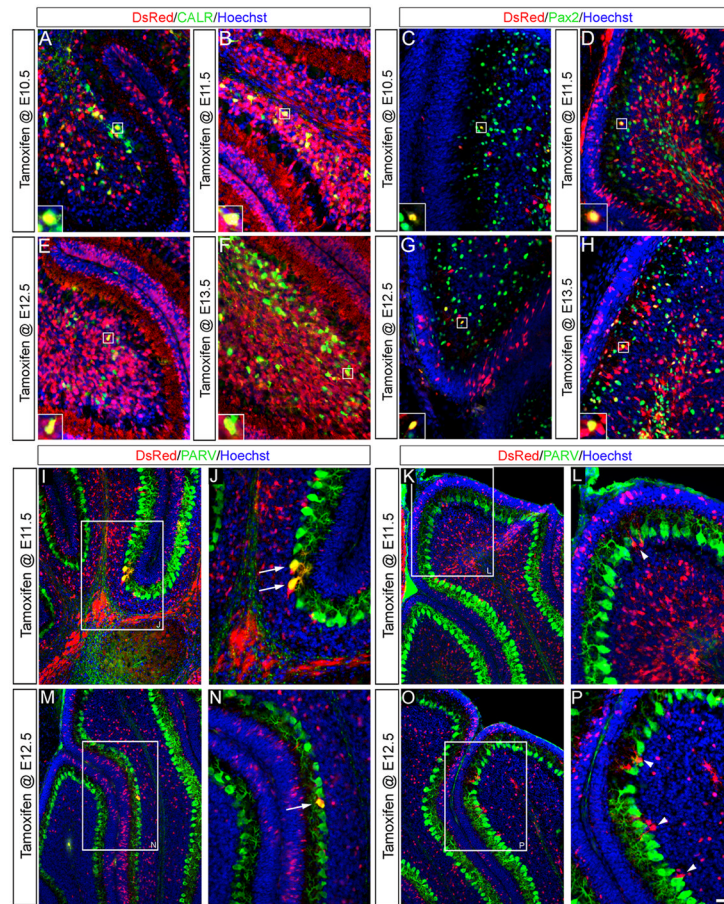
Fig. 10. Molecular analysis of the *Wnt1* lineage in the developing Cb cortex
(**A,B,E,F**) ICC with antibodies that recognized tdTomato (DsRed, red) or Calretinin (CALR, green) on P7 sagittal sections uncovered that *Wnt1* expressing progenitors (red) contributed to unipolar brush cells (green) in folia IX and X. (**C,D,G,H**) Antibody labeling against PAX2 (green) showed that the *Wnt1* lineage gave rise to inhibitory interneurons of the granular layer. (**I–P**) ICC with Parvalbumin (PARV, green) revealed that the *Wnt1* lineage contributed to scattered Purkinje cells (arrows) and Bergmann glia (arrowheads). Scale bar, 61 μm.
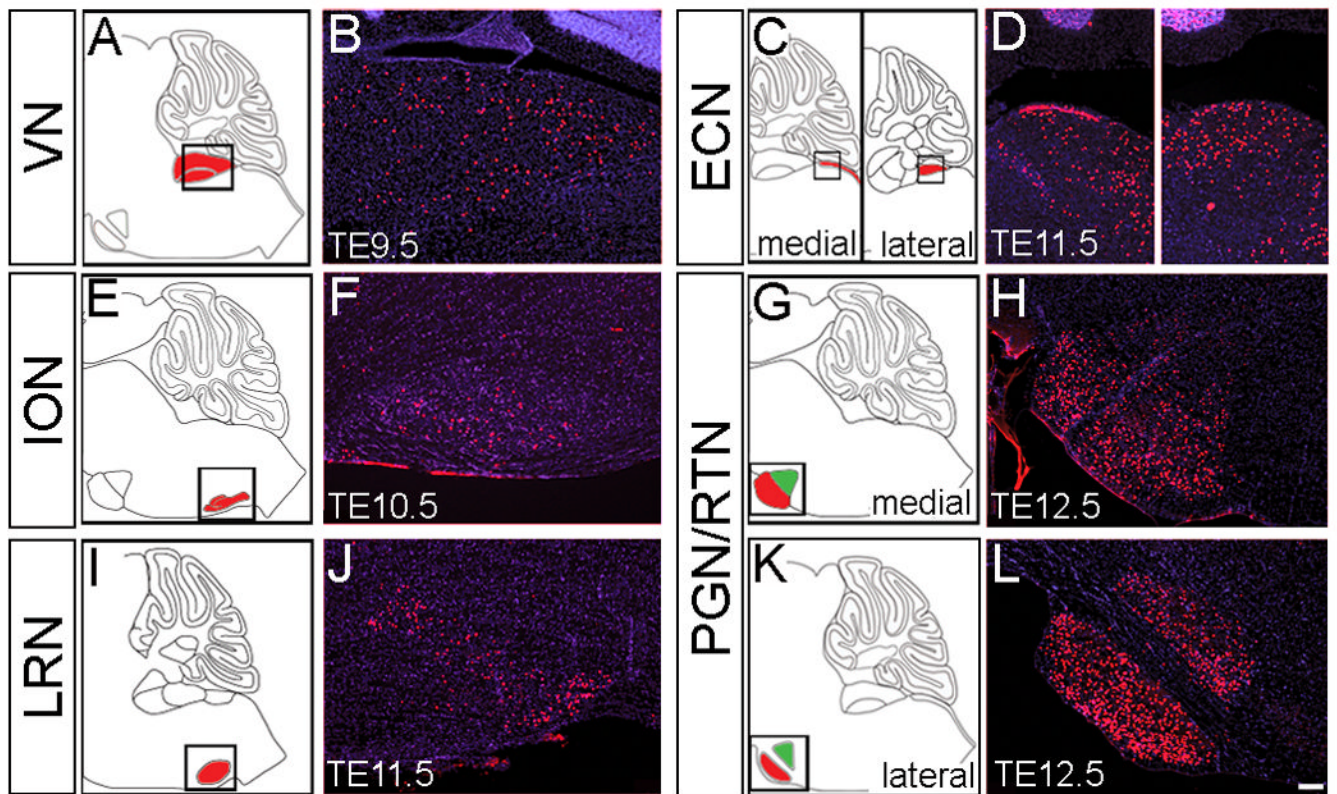
Fig. 11. The temporal dissection of the *Wnt1* lineage contribution to the precerebellar system
(A,C,E,G,I,K) Sagittal schematics illustrate the section plane used to analyze each precerebellar nuclei. The VN (A), ECN (C), ION (E), PGN (G,K) and LRN (I) are depicted in red and the RTN (G,K) in green. The imaging frame is delineated by the box.
(B,D,F,H,J,L) ICC on adult sagittal sections with antibodies against β-gal (red) revealed that *Wnt1* expressing progenitors (red) contributed to all six precerebellar nuclei and the magnitude of this contribution shifted across development. **(A,B)** In the VN, the onset of *Wnt1* contribution was at E8.5 with peak marking from E9.5-E11.5; E9.5 is shown. **(C,D)** In the ECN, the onset of *Wnt1* contribution was at E8.5 with a broad peak in marking from E9.5-E13.5; E11.5 marking is shown. **(E,F)** In the ION, *Wnt1*-derived neurons were observed with marking at E10.5 and E11.5. **(G,H)** The PGN had a peak contribution from the *Wnt1* lineage marked at E12.5. **(I,J)** In the LRN, the onset of *Wnt1* contribution was at E9.5 with peak marking from E10.5-E13.5. **(K,L)** The peak contribution to the lateral PGN and RTN was at E12.5. Scale bar: 120 μm.